ISSN 1070-3284, Russian Journal of Coordination Chemistry, 2020, Vol. 46, No. 7, pp. 443–457. © Pleiades Publishing, Ltd., 2020.
Russian Text © The Author(s), 2020, published in Koordinatsionnaya Khimiya, 2020, Vol. 46, No. 7, pp. 387–401.

Dedicated to I.L. Eremenko on the occasion of his 70th birthday

Main Approaches to the Synthesis of Heterometallic Metal-Organic Frameworks

A. A. Sapianik[a, b] and V. P. Fedin[a, b, *]

[a] *Nikolaev Institute of Inorganic Chemistry, Siberian Branch, Russian Academy of Sciences, Novosibirsk, 630090 Russia*
[b] *Novosibirsk National State Research University, Novosibirsk, 630090 Russia*
**e-mail: cluster@niic.nsc.ru*

Received January 16, 2020; revised January 30, 2020; accepted January 31, 2020

Abstract—The chemistry of metal-organic frameworks (MOF) is intensively developed during the recent years. Such compounds form unique porous structures and demonstrate very interesting functional properties: selective sorption and magnetic, catalytic, luminescence, and many other characteristics. The most part of the studied MOF is homometallic. The heterometallic MOF are studied to a lower extent. Nevertheless, the introduction of a heterometal makes it possible to purposefully modify the properties of the already known structures and also to prepare basically new structures. The results of studies of the synthesis methods of the heterometallic MOF are generalized and reviewed. The main structural types of these compounds and their functional properties are considered.

Keywords: coordination polymers, porous carcass structures, synthesis, structure, heterometallic complexes
DOI: 10.1134/S1070328420060093

INTRODUCTION

Metal-organic frameworks (MOF) represent a new class of porous materials consisting of inorganic secondary building units, which are connected by organic ligands (linkers). Numerous materials based on MOF have been reported since the first reports on MOF in the 1990s [1]. Their outstanding and unique properties resulted in increasing interest in these materials. Porous MOF combining several functions (such as porosity and magnetism, porosity and luminescence) evoke huge interest due to wide possibilities of the structural design and application for "green" resource-saving power engineering (for example, hydrogen or methane storage, as well as CO_2 trapping), luminescence sensing, development of new magnetic materials, etc.

The preparation of new porous carcasses with specified properties is a complicated task, since the functional properties will be determined by the type of mutual bonding of inorganic and organic fragments in the final structure, which is often difficult to predict. Therefore, the key role belongs to the choice of building blocks for units of the MOF carcass of molecular complexes with the already known geometry. Along with the adsorption properties, other functional properties of hybrid porous MOF are usually caused by metal ions (for example, for magnetic and luminescent materials). In this case, a special place is occupied by heterometallic building blocks, since they allow one to more finely vary functional features caused by the metal cations in the structure, for instance, the heterometallic 3*d*–4*f* MOF can act as either "single-molecule" magnets, or luminescent sources of the white color [2].

A combination of several functional features in one structure attracts increasing interest of the scientific society in the recent years. The introduction of the molecules with several linkers [3, 4] or several different metals into one carcass [5, 6] or a combination of these two approaches [7] is a powerful approach for the development of the MOF-based materials. Thus, the obtained materials are more specialized for specific applications or can be used as multifunctional materials for simultaneous performing various tasks. Mixing of diverse metals is an important concept of heterogeneous catalysis. The synergetic effect of additional types of metals is known for enzymes in the nature, and the heterometallic catalysts are widely used in the very diverse catalytic reactions [8]. Therefore, joining of several metals into one MOF structure should improve the properties of the prepared material.

The term "heterometallic MOF" is applied to several various types of metal-organic polymeric structures: several cations of different metals are compo-

nents of the secondary building block; cations of different metals are components of different secondary building blocks joined into one MOF structure; cations of different metals are components of different structure-forming moieties, namely, cations of some metals exist in the metallocenter, and cations of the heterometal exist in the metalloligand; and finally, the metal cations different from those in the charged carcass can be included into the cavities as supramolecular guests. Several main approaches for the preparation of the heterometallic MOF have been accomplished to the present time:

(1) post-synthetic modification of MOF due to the inclusion of ions of other metals into the carcass pores or post-synthetic modification with the substitution of some cations in the carcass by other cations with a close ion radius;

(2) using salts of several metals in the initial reaction mixture to obtain heterometallic analogues of the known homometallic structures, where cations of various metals occupy equivalent structural positions;

(3) using the metalloligand containing a metal cation different from the structure-forming metal of the carcass;

(4) using multicomponent mixtures (containing sources of at least two different metal cations) with the purpose of including these cations into the structure. In this case, there were attempts to prepare quite novel structures unlike the method indicated in point (2);

(5) using the pre-synthesized polynuclear heterometallic complexes for the preparation of MOF with the specified geometry of the nodes.

Each approach will be considered in more detail.

POST-SYNTHETIC MODIFICATION

The method of the post-synthetic modification of carcasses has already been developed widely in the chemistry of MOF. Organic linkers are usually modified using this method due to performing reactions on functional groups of these ligands for the modification of the functional properties of the polymers. Nevertheless, the composition of MOF can be modified by metal cations using the post-synthetic approach. Several basically different mechanisms can be distinguished.

In the first case, metal cations occupy certain positions in channels/cavities of the earlier obtained porous MOF. Here the retention of the metal cation in the certain position occurs due to the interactions between the donor atoms of the organic linker and introduced metal cation. The preparation of the homometallic MOF $[Ga(OH)(Btec)] \cdot 0.5H_2O$, where H_4Btec is 1,2,4,5-benzenetetracarboxylic acid (MIL-61), was reported [9]. Since the initial carcass is a rigid structure having channels and free carboxyl groups, it turned out to be possible to include Tb^{3+} and Cu^{2+} cations by the post-synthetic treatment of the carcass with solutions of the corresponding metal salts. The preparation of the heterometallic MOF made it possible to substantially modify the functional properties of these MOF for the diagnostics of prostate cancer due to the detection of sarcosine molecules. An additional inclusion of Cu^{2+} cations controls the luminescence of Tb^{3+} due to the ligand–metal charge transfer and also provides accessible regions for the coordination of sarcosine in the channels, resulting in a substantial decrease in the efficiency of the charge transfer and luminescence quenching upon the inclusion of sarcosine. Continuing the studies of metal cation inclusion into MIL-61 [10], the authors obtained a series of inclusion compounds with various lanthanide cations Ln-dopd-MIL-61 (Ln = Eu^{3+}, Tb^{3+}, Sm^{3+}, Dy^{3+}). In addition to the characteristic luminescence of Eu^{3+} and Tb^{3+}, Sm-MIL-61 and Dy-MIL-61B were shown to exhibit very weak luminescence properties. Nevertheless, in the presence of silver cations in an aqueous solution, a substantial luminescence rise is observed for Sm^{3+} and Dy^{3+}, which can be used for the production of sensor materials for the determination of the concentration of silver ions.

The carcass based on Zr^{4+} and 1,2,4,5-benzenetetracarboxylic acid was used as the initial MOF [11]. First, Eu^{3+} cations and then Cu^{2+}, which are distributed over the surface of the carcass pores, were included according to the already described scheme. This modification made it possible to carry out the selective detection of uric thioglycolic acid, which is a biomarker of the cancerous vinyl chloride monomer in the human organism. One of the key features is a very low detection limit (89 ng/mL) and high luminescence intensity upon the inclusion of the analyte.

The procedure of the synthesis of HKUST-1 ($[Cu_3(Btc)_2]$, where H_3Btc is 1,3,5-benzenetricarboxylic acid) was modified [12] for the preparation of the heterometallic analogue. The doping agents were $Zn(OAc)_2 \cdot 2H_2O$, $RuCl_3 \cdot xH_2O$, and $Pd(OAc)_2$. It was demonstrated that the synthesis without a solvent is an appropriate and easy route for the preparation of the heterometallic analogue HKUST-1 in such a way that the content of the doping metal cation can be monitored by the ratio of the initial reactants in the mixture. All synthesized compounds are characterized by a high crystallinity and permanent porosity. The inclusion of metal cations of the second type made it possible to substantially improve the electrocatalytic activity in the reduction of CO_2.

The substitution of metal cations in the structures of the synthesized MOF is an alternative mechanism of the post-synthetic modification for the preparation of heterometallic carcasses. This substitution is usually characteristic of cations with close sizes. A particular case of this substitution is the replacement of hydroxonium cations, which compensate the negative charge of the anionic carcass. For example, we showed [13]

that the hydroxonium cation can completely be replaced by various alkaline metal cations in the anionic MOF $(H_3O)_2[Zn_4(Ur)(HFdc)_2(Fdc)_4]$ (Ur is urotropine, H_2Fdc is furan-2,5-dicarboxylic acid) (Fig. 1). In turn, this affects the luminescence intensity of the samples and quantum yields and serves as the basis for the development of sensors for alkaline metals.

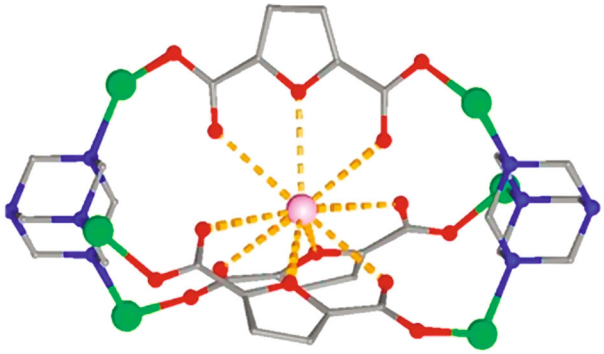

Fig. 1. Cryptand-like cavity in the structure of $M_2[Zn_4(Ur)(HFdc)_2(Fdc)_4]$ containing zinc cations (green-colored) and alkaline metal cation (pink-colored). Adapted with permission from [13]. Copyright 2017, Wiley-VCH.

USE OF SALTS OF SEVERAL METALS IN THE INITIAL REACTION MIXTURE

This method for the preparation of the heterometallic MOF is the use of salts of different metals in the initial reaction mixture for the preparation of heterometallic analogues of the already known homometallic structures. This approach is often used for the modification of the properties in the known MOF, in particular, for changing the magnetic behavior.

The preparation of the bimetallic derivatives MOF-5 ($[Zn_4O(Bdc)_3]$ (H_2Bdc is 1,4-benzenedicarboxylic acid, and zinc nitrate and iron(III) acetylacetonate in the initial mixture are used in the synthesis) is reported [14]. The obtained structure has the morphology of MOF-5, and the zinc and iron cations occupy equivalent positions and are uniformly distributed in the structure. The introduction of Fe^{3+} ions into MOF-5 produces coordinately unsaturated sites, which results in the predominant sorption of water molecules with respect to ethanol molecules. The porous structure of Fe(III)-MOF-5 provides the free diffusion of water molecules. Thus, the materials based on this heterometallic compound are interesting for the production of highly selective membranes. For a model system of an aqueous solution of ethanol (90 wt %), the hybrid membrane containing Fe(III)-MOF-5 demonstrates the highest efficiency of water and ethanol separation with a separation coefficient of 3423 and the penetration flow rate equal to 1540 g m^{-2} h^{-1}, which are much higher than those of the hybrid membranes based on the homometallic MOF-5.

A mixture of $Co(NO_3)_2 \cdot 6H_2O$, $Zn(NO_3)_2 \cdot 6H_2O$, and methylimidazole in methanol was used for the preparation of the heterometallic MOF with various metal ratios in the structure [15]. Then the MOF was subjected to pyrolysis, and the obtained material containing Co_3O_4/ZnO exhibits considerably higher catalytic characteristics for glycerol carbonylation compared to the corresponding oxides prepared from the homometallic MOF. In particular, the yield on the $Co_{50\%}Zn_{50\%}$ catalyst reached 85% with the 93% conversion and a selectivity of ~91%. This catalytic efficiency is substantially higher than that of the most part of other heterogeneous catalysts. A mixture of the metal salts was also used [16] for the preparation of the heterometallic MOF. Here Zn^{2+} or Cu^{2+} cations occupy the sites of the Mn^{2+} cations in the structure of STU-2[Mn(BIm)] (BIm is 1,2-bis((5*H*-imidazol-4-yl)methylene)hydrazine) [17, 18]. Doping resulted in the improvement of the catalytic activity of the cyanosilylation of various aromatic aldehydes for $Zn_{0.29}$-STU-2 at room temperature.

The family of the heterometallic analogues MOF-74 $[M_2(Dhtp)(H_2O)_2]$ (M = Mg, Mn, Fe, Co, Ni, and Zn; Dhtp is 2,5-dihydroxyterephthalate anion) was obtained [19]. The Co-, Fe-, and Ni-MOF-74 demonstrate weak ferromagnetic interactions between the chains of the metal atoms in the structure. It was shown that NiFe-MOF-74 was characterized by the ferromagnetic ordering. The introduction of Fe^{3+} cations makes it possible to modulate the onset of spontaneous magnetization between 10 and 16 K due to the controlled appearance of antiferromagnetic interactions between the chains (Fig. 2).

An interesting example is presented in [20]. The researchers attempted to obtain the heterogeneous crystal consisting of two related polymers ZIF-8/67($[M(2\text{-}MIm)_2]$, where M = Zn for ZIF-8 and Co for ZIF-67, and 2-MIm is 2-methylimidazole) rather than the simple heterometallic carcass. When Co^{2+} and Zn^{2+} ions exist in the initial reaction solution, the homogeneous distribution of two metals is achieved only at a high Co/Zn ratio, whereas the concentration gradient from the cobalt-enriched cores to the shells enriched in zinc is observed at a low Co/Zn ratio.

USE OF METALLOLIGANDS

This method for the synthesis of the heterometallic MOF is the use of the metalloligand containing the metal cation different from the structure-forming metal of the carcass.

The heterometallic In/Pd MOF were obtained [21], where the In^{3+} cations exist in the trinuclear

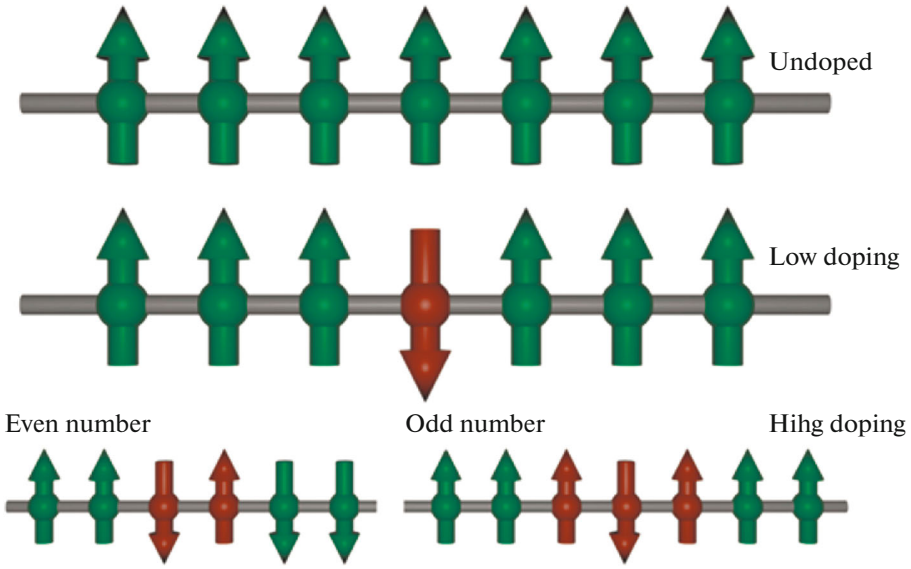

Fig. 2. Proposed changes in the spin configuration of the magnetic chains in MOF-74 upon doping with iron. Nickel is green-colored, and iron is orange. Reprinted with permission from [19]. Copyright © 2017 by the American Chemical Society.

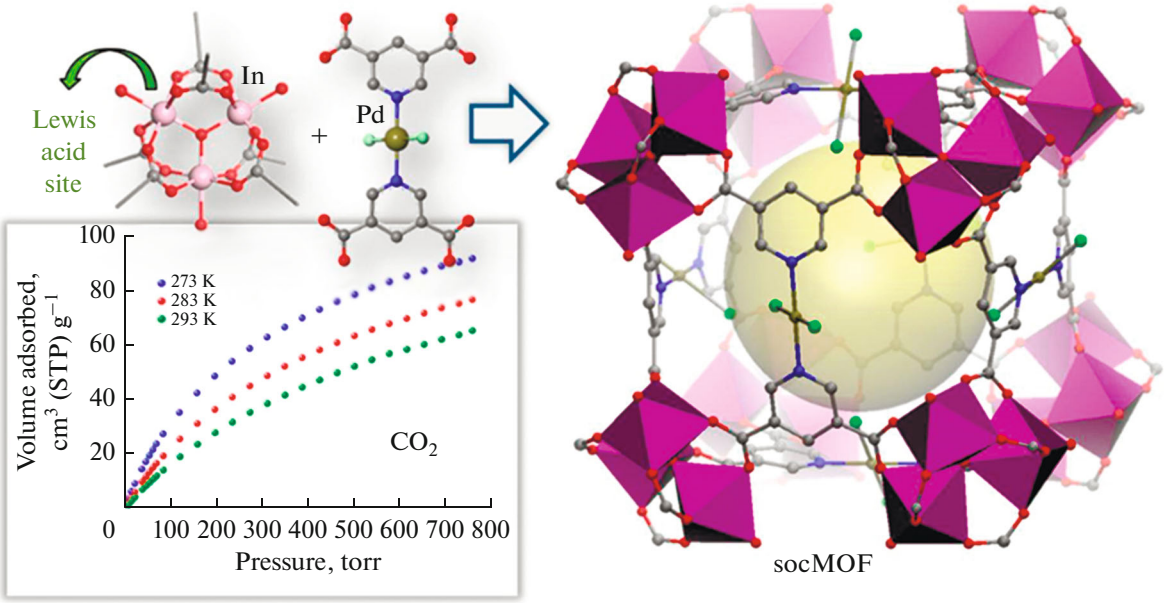

Fig. 3. Node $\{In_3O(COO)_6\}$ and metalloligand *trans*-$[PdCl_2(Pdc)_2]$ in the structure of the MOF and carbon dioxide sorption at various temperatures. Reprinted with permission from [21]. Copyright © 2018 by the American Chemical Society.

hexacarboxylate node $\{In_3O(COO)_6\}$ and palladium is included into the metalloligand *trans*-$[PdCl_2(Pdc)_2]$ (H_2Pdc is pyridine-3,5-dicarboxylic acid). The $[In_3O(Pdc)_{1.5}(H_2O)_2Cl]$ carcass is three-dimensional and permanently porous showing the high gravimetric (92.3 cm^3 g^{-1}) and volumetric (120.9 cm^3 cm^{-3}) capacities with respect to CO_2 sorption at 273 K and 1 bar (Fig. 3), as well as the high selectivity for the separation of a CO_2/CH_4 mixture (selectivity factor 15.4 for a 50 : 50 molar mixture) and a CO_2/N_2 mixture (selectivity factor 131.7 for a 10 : 90 molar mixture) with a moderate heat of adsorption for CO_2

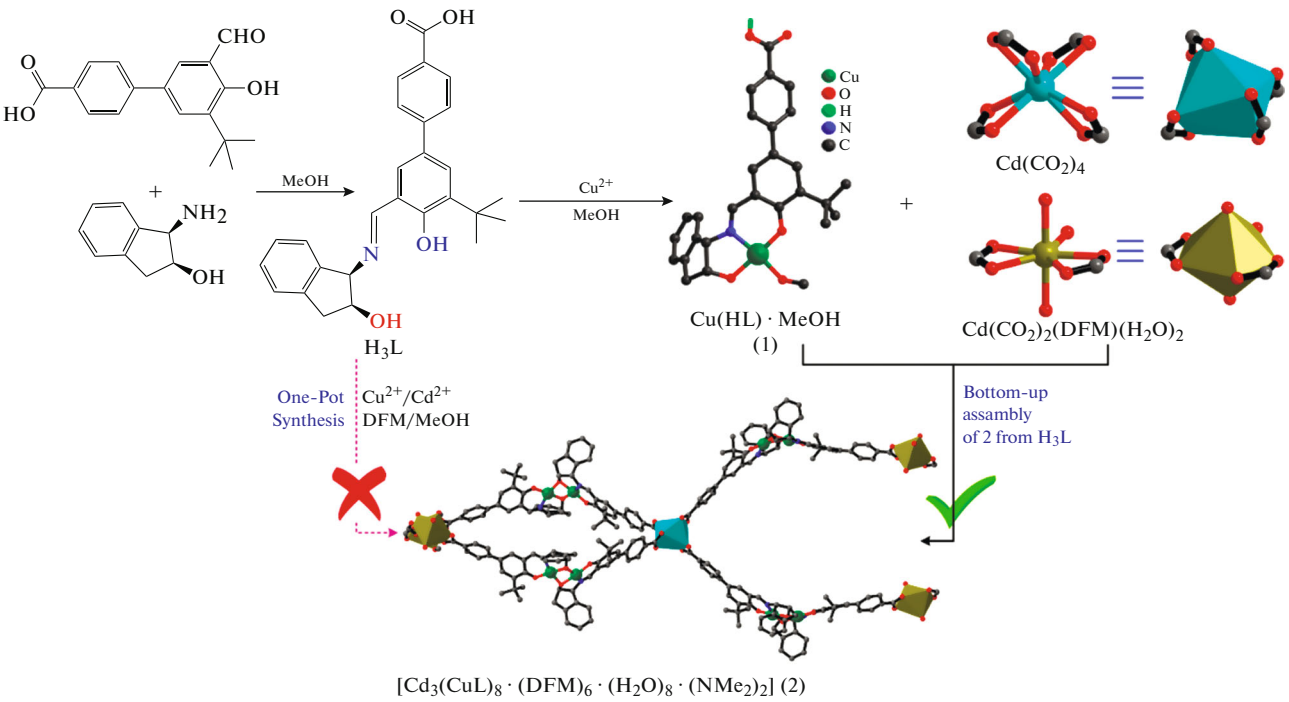

Fig. 4. Scheme of the synthesis of the MOF $[Cd_3(CuL)_8(Dmf)_6(H_2O)_8(NMe_2)_2]$. Reprinted with permission from [22]. Copyright © 2018 by the American Chemical Society.

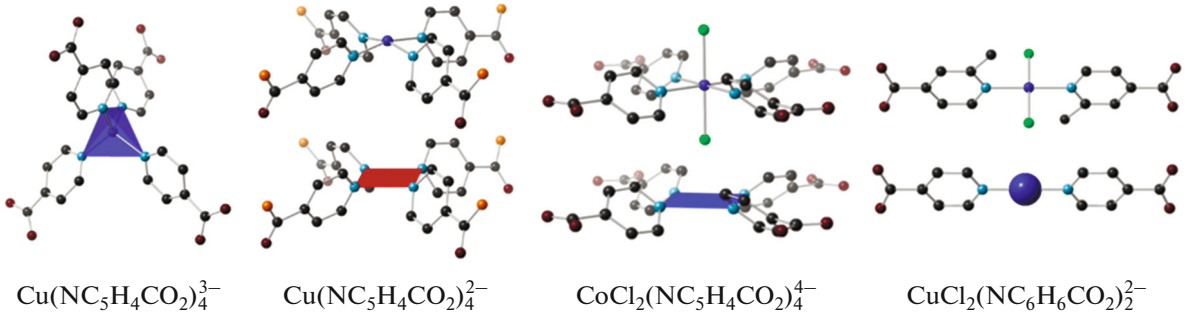

Fig. 5. Published metalloligands. Adapted with permission from [23]. Copyright © 2018 by the American Chemical Society.

(29.8 kJ/mol). The second carcass $[(Me_2NH_2)In(Pdc)]$ is also three-dimensional with the topology of platinum sulfide PtS.

The metalloligand in [22] was [Cu(HL)] (Fig. 4), which reacts with cadmium bromide to form 2D-MOF $[Cd_3(CuL)_8(Dmf)_6(H_2O)_8(NMe_2)_2]$ serving as the heterogeneous catalyst in the Henry and Friedel–Crafts reactions.

The work [23] is interesting from the topological point of view. The tetra- and dicarboxylate ligands based on copper and cobalt were used as the building blocks (Fig. 5). Their combination with the clusters $[Zr_6(\mu^3\text{-}O)_4(\mu^3\text{-}OH)_4(CO_2)_{12}]$ and $[Hf_6(\mu^3\text{-}O)_4(\mu^3\text{-}OH)_4(CO_2)_{12}]$ made it possible to obtain eight new heterometallic MOF with a complicated topology.

Similar dipyrrin (Dpm) metalloligands based on cations of various metals (Scheme 1) [24] in the reactions with cadmium chloride gave several heterometallic MOF $[\{M(Dpm)_2\}_2CdCl_2(Solv)_x]$. A distinctive feature from the previous work is that the ligands contain the N-donor atom in the aromatic ring instead of the carboxyl group and the zinc and cadmium cations are bound in the three-dimensional carcass only due to the N-donor ligands. It is also important that the obtained carcasses can be synthesized from a mixture of metal salts and dipyrrin linkers.

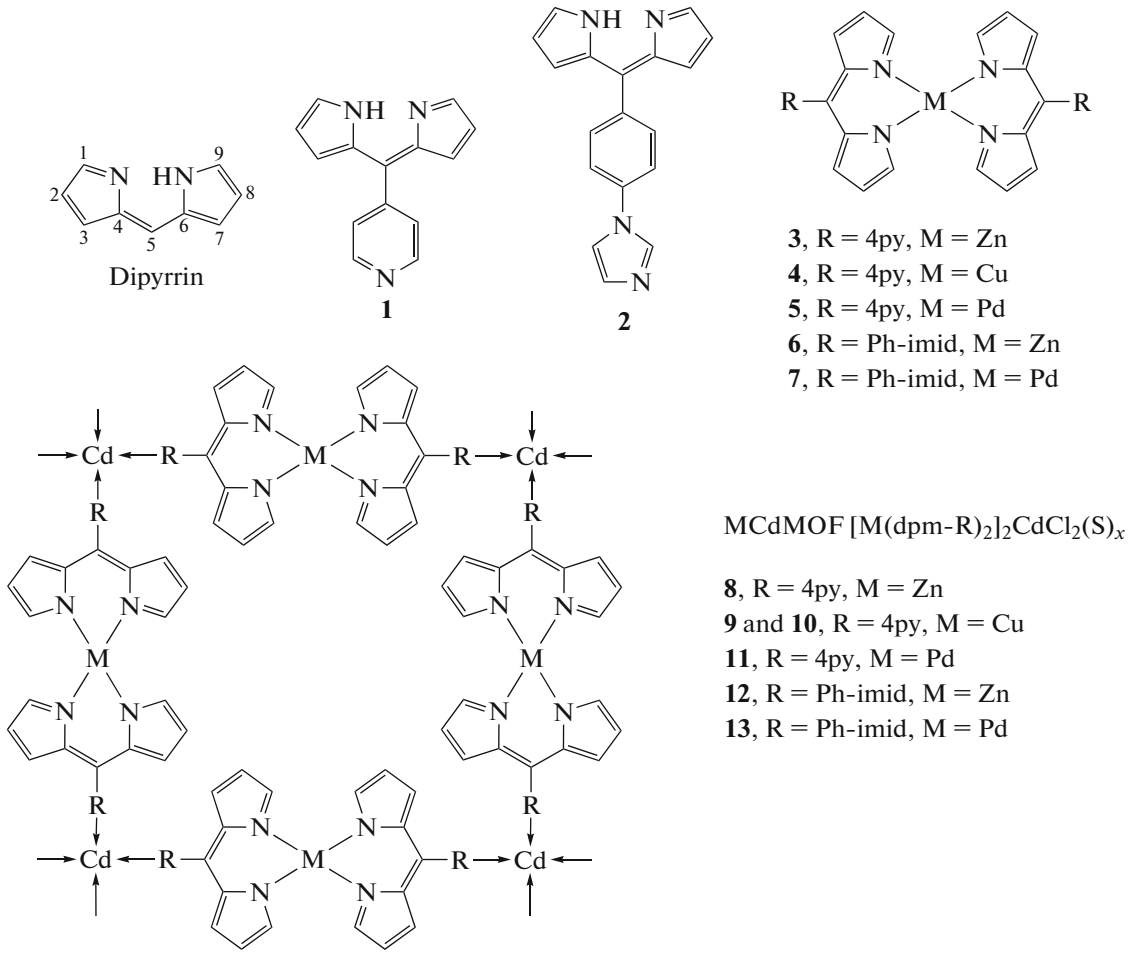

Scheme 1. Dipyrrin ligands **1** and **2** and metalloligands **3**–**7** used for the synthesis of MCdMOF **8**–**13**. Reprinted with permission from [24]. Copyright © 2013 by the American Chemical Society.

USE OF MULTICOMPONENT MIXTURES FOR THE SYNTHESIS OF NEW HETEROMETALLIC MOF

One more method that provides the preparation of heterometallic MOF is the use of multicomponent mixtures containing sources of at least two different metal cations. This approach does not allow one to exactly predict whether heterometallic nodes would be formed or cations of various metals would be isolated and separated from each other in the structure to form different types of homometallic nodes. Nevertheless, this practically simple method is used most frequently.

The heterometallic MOF [$\{Yb_6Cu_{12}(OH)_4(Pyc)_{12}(H_2O)_{36}\} \cdot (NO_3)_{14} \cdot xS$] (QUST-81) and [$\{Yb_4O(H_2O)_4Cu_8(OH)_{8/3}(Pyc)_8(HCOO)_4\} \cdot (NO_3)_{10/3}$] (QUST-82) ($H_2Pyc$ is 1*H*-pyrazole-4-carboxylic acid) were first used for the efficient removal of heterocyclic sulfur-containing organic compounds from motor fuel [25]. The MOF QUST-81 was synthesized by heating a mixture of Yb(III) and Cu(II) nitrates with pyrazole-carboxylic acid in a dimethylformamide–dimethylacetamide–*N*-methyl-2-pyrrolidone mixture at 100°C under the solvothermal conditions. The MOF QUST-82 was obtained by the repeated heating of the crystals of QUST-81 in the initial reaction mixture at 120°C. The structures of both coordination polymers contain nodes of two types. In the case of QUST-81, these are $\{Yb_2(COO_4)_4(H_2O)_8\}$ and $\{Cu_3(OH)(PyC)_3\}$. For QUST-82, these are $\{Yb_4O(COO)_8(H_2O)_4\}$ and $\{(Cu_3(OH)(PyC)_3)_8(HCOO)_{12}\}$. The nodes are linked to form three-dimensional porous carcasses.

The $[Zn_2(L)K_2(\mu^2\text{-}H_2O)_2(\mu^2\text{-}SCN)_4]$ compound (H_2L is bis(pyridine-2-aldehyde) thiocarbazone) [26] was obtained from a mixture of zinc acetate, potassium thiocyanate, and H_2L in methanol on heating. The structure contains metal cations of two types, which are not bound to each other by carboxylate bridges but form the homometallic nodes $\{K_2(\mu^2\text{-}H_2O)_2\}$ of two types, and zinc cations in the tetrahedral environment of the donor atoms of the ligands.

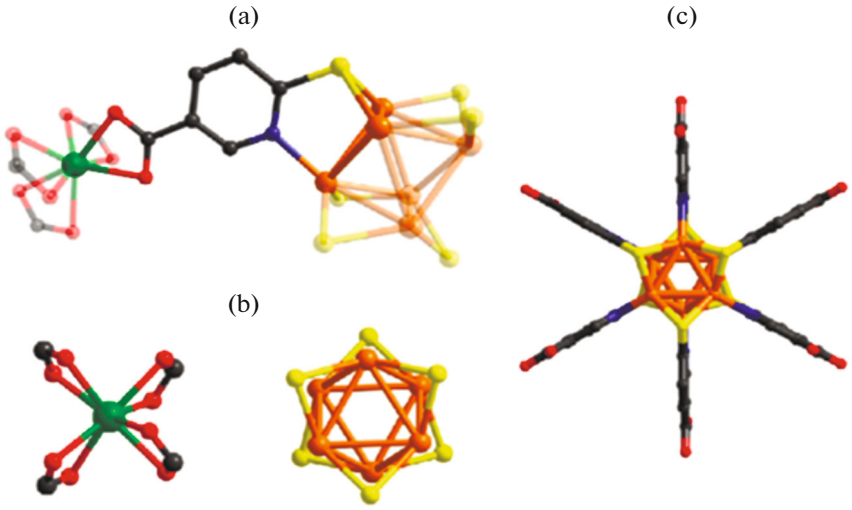

Fig. 6. (a) Coordination environment of ligand L^2, (b) four-bonded node $In(COO)_4$ and cluster $\{Cu_6S_6\}$, and (c) hexadentate metalloligand in the structure of $\{[(CH_3)_2NH_2]InCu_4L_4 \cdot MeCN \cdot H_2O\}$. Reprinted with permission from [30]. Copyright © 2016.

Four new heterometallic MOF $[Zn_4Ln_2(Imdc)_4(SO_4)(H_2O)_8] \cdot 4H_2O$ (Ln = Nd, Sm, Eu, and Gd; H_3Imdc is imidazole-4,5-dicarboxylic acid) were synthesized hydrothermally in the reactions of Ln_2O_3 with imidazole-4,5-dicarboxylic acid and $ZnSO_4 \cdot 7H_2O$ [27]. As in the previous cases, the metal cations form no heterometallic nodes but are isolated from each other at the linker length. The carcass contains two structurally independent zinc cations differed in the coordination number (coordination numbers 4 and 6). The lanthanide cation is coordinated by nine oxygen atoms of the carboxyl groups of the ligand and coordinated water molecules. An interesting feature of the obtained heterometallic compounds is the possibility of the selective detection of I^- in the solution due to luminescence quenching.

The MOF $[H(H_2O)_8][DyZn_4(Imdc)_4(Im)_4]$ (H_3Imdc is 4,5-imidazoledicarboxylic acid, and Im is imidazole) [28] demonstrate the possibility of varying the luminescence properties depending on the excitation wavelength, including showing white luminescence. The synthesis was carried out from dysprosium chloride and zinc acetate. The metal cations were isolated in the structure by the imidazoledicarboxylate anions. The MOF $(Me_2NH_2)_5[In_3Zn_6(\mu^3\text{-}OH)_2(Bptc)_6]$ was synthesized [29] from indium and zinc nitrates in the reaction with biphenyl-3,3',5,5'-tetracarboxylic acid (H_4Bptc). The structure contains secondary building homometallic blocks of two types: $\{In(COO)_4\}$ and $\{Zn_3(\mu^3\text{-}OH)(CO_2)_6\}$. The three-dimensional structure of the carcass contains a system of cavities providing the possibility of gas sorption, storage, and separation. The surface area measured by the BET method was 1200 m^2/g, and the selectivity of separation of C_2H_2/N_2 and CO_2/N_2 gas mixtures (vol : vol = 15 : 85) was 103.2 and 17.0, respectively, at 1 atm and 273 K.

Indium(III) chloride and copper(I) iodide were used for the production of the heterometallic MOF $[(CH_3)_2NH_2)InCu_4L_4] \cdot MeCN \cdot H_2O$ (H_2L is 6-mercapropyridine-3-carboxylic acid) [30]. The structure contains the homometallic nodes of two types: mononuclear $\{In(COO)_4\}$ and homonuclear $\{Cu_6S_6\}$ (Fig. 6). Owing to its porous structure and anionic type of the carcass, the compound demonstrates the possibility of the selective separation of C_2 hydrocarbons from methane and also can sorb mercury(II) from an ethanolic solution.

The MOF $(H_3O)_3[Gd_3Mn_2(Trz)_4] \cdot 12H_2O$ (H_4Trz is tris(1*H*-tetrazol-5-yl)methanol) contains the hexanuclear cluster $\{Gd_6O_8\}$ [31]. The crystals of this compound were obtained by mixing $GdCl_3 \cdot 6H_2O$, $MnCl_2 \cdot 4H_2O$, KC_4N_3, NH_4F, NaN_3, H_2O, and MeOH (vol : vol = 3 : 1), and the resulting mixture was heated at 145°C for 3 days. The magnetic measurements show that the compound is a good candidate to the role of magnetic heat carriers in a low-temperature field.

The examples in which the polynuclear secondary building block contains at least two different metal cations are further considered. Attention is focused [32] on the family of the heterometallic MOF, which can hardly be obtained, since they consist of the metal ions with strongly different properties, for example, Mg^{2+} and V^{3+} or Ni^{2+} and In^{3+}. An important feature of the synthesis is the use of a large excess M^{2+} cation salt, since an X-ray amorphous product is formed when the metal ratios close to the equimolar one are used. The metal cations occupy crystallographically equivalent sites. The metal cations in the structure form the trinuclear node $\{M^{II}_2M^{III}(\mu^3\text{-}OH)(CO_2)_6\}$ (Fig. 7), and the three-dimensional structure of the synthesized MOF CPM-200 contains a system of

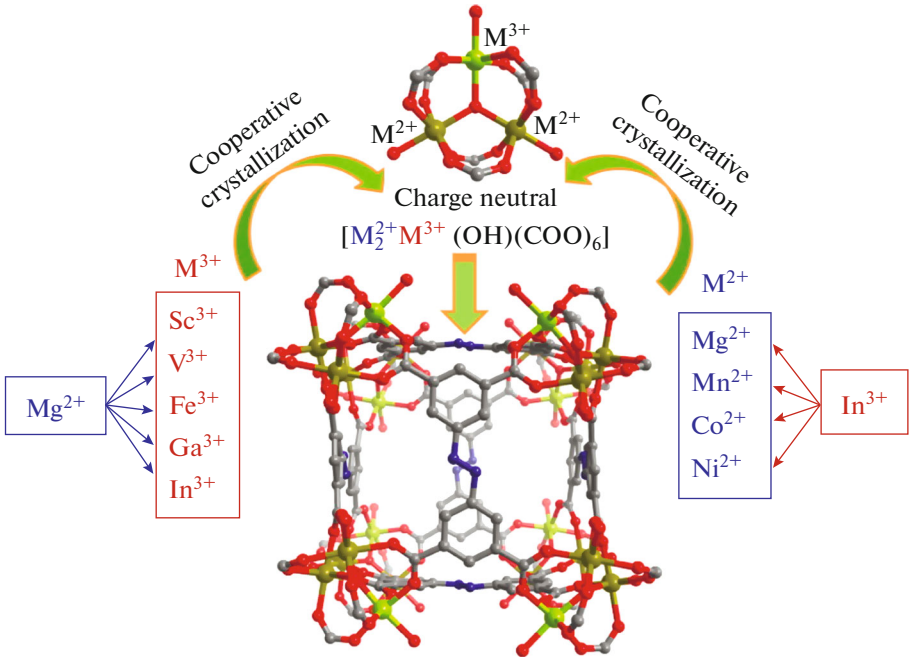

Fig. 7. General scheme of the synthesis of the $\{M_2^{II}M^{III}(\mu^3\text{-OH})(CO_2)_6\}$ node in the structure of the heterometallic CPM-200 MOF. Reprinted with permission from [32]. Copyright © 2016 by the American Chemical Society.

channels. The compounds demonstrate a high porosity (BET from 877 to 1459 m^2/g) and can be used as sorbents for CO_2 and H_2 storage.

The electrocatalytic oxygen evolution in a 0.1 M KOH electrolyte was conducted [33] on the basis of the isostructural hetero- and homometallic MOF $[NH_2(CH_3)_2][M_3(\mu^3\text{-OH})(H_2O)_3(Bhb)]$ (M_3 = Co_3, Co_2Ni, $CoNi_2$, and Ni_3; H_6Bhb is 4,4',4"-benzene-1,3,5-triylhexabenzoic acid). It was shown that the kinetics for the bimetallic catalysts was more efficient compared to that of their homometallic analogues. The heterometallic blocks $\{M_2M'O(COO)_6\}$ were prepared from the metal salts taken in a stoichiometric ratio.

A series of homo- and heterometallic MOF was synthesized from the trimesate anion [34]. An interesting structural feature of these compounds is the spiral rotation axis, and correspondingly, all carcasses crystallize in the chiral symmetry group (Fig. 8). The compounds $[Zn(HBtc)(H_2O)]$, $Li_4[Cd_2(HBtc)(Btc)_2]$, $[CoLi(Btc)(Dma)_2]$, $[CdLi_2(Btc)_{4/3}(H_2O)_3]$, and $Li_2[Zn_3Li_5(Btc)_4(Mtaz)(H_2O)_4]$ (Mtaz is 5-methyltetrazole) were synthesized with the variation of the ratio of the initial metal salts in the reactions with organic ligands under the solvothermal conditions. The chiral crystals based on Cd(II) and Zn(II) demonstrate interesting nonlinear optical properties.

The rigid asymmetric tricarboxylate ligand (H_3L is *p*-terphenyl-3,4",5-tricarboxylic acid) was used [35] for the preparation of the heterometallic alkaline-earth–lanthanide microporous luminescent MOF $[Ba_3La_{0.5}(\mu^3\text{-L})_{2.5}(H_2O)_3(Dmf)] \cdot 3DMF$. The synthesis was carried out from a mixture of metal nitrates with acid H_3L in a DMF–H_2O (1 : 1) solution with the addition of a minor amount of nitric acid under the solvothermal conditions. The structure contains barium cations of three types differed by the coordination environment and the lanthanium cations of one type. These cations form the heterometallic framework in the structure (Fig. 9). The luminescence response to the inclusion of various cations from aqueous solutions was studied for the synthesized compound. It turned out that the inclusion of Al^{3+} cations and MnO_4^- anions results in the partial luminescence quenching already at sufficiently low concentrations (10^{-3} and 10^{-4} mol/L, respectively).

The heterometallic MOF $[In_{0.5}K(3\text{-Qlc})Cl_{1.5}(H_2O)_{0.5}]_{2n}$ and $[InK(Ox)_2(H_2O)_4]$ (3-HQlc is quinoline-3-carboxylic acid, and H_2Ox is oxalic acid) [36] were synthesized from KOH and indium(III) chloride or nitrate, respectively. The structures of both MOF contain the heterometallic node (Fig. 10). The obtained compounds demonstrate a change in the solid-state luminescence from blue to yellow and white with a temperature change.

In a series of the isostructural MOF $[Ln_2Ni(OAc)_5(HL)(L)]$ (H_2L is 2-hydroxyimino-*N*-[1-(2-pyrazinyl)ethyldiene]propanohydrazone; Ln = Dy, Tb, and Gd) [37], the coordination node is heterometallic and the cations of various metals are bound to each other via the bridging oxygen atom. The com-

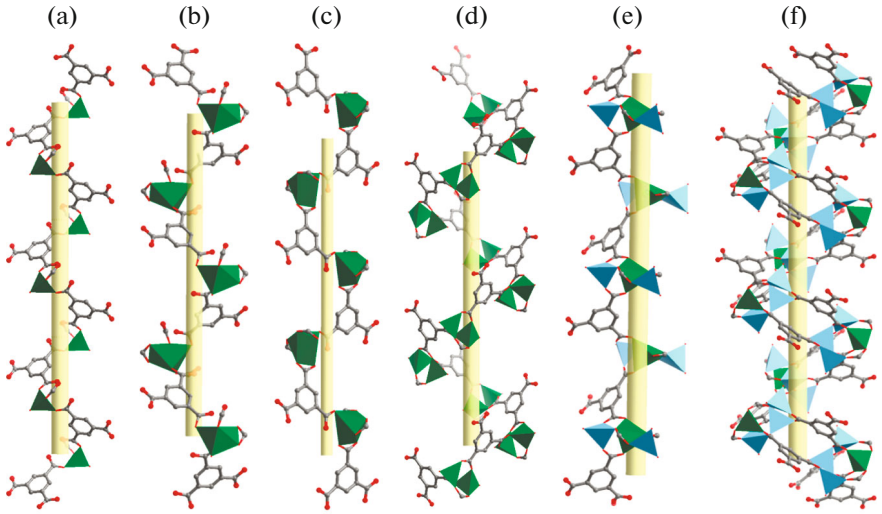

Fig. 8. Six types of spiral chains in the structures [34]: (a) $[Zn(HBtc)(H_2O)]$, (b, c) $Li_4[Cd_2(HBtc)(Btc)_2]$, (d) $[CoLi(Btc)(Dma)_2]$, (e) $[CdLi_2(Btc)_{4/3}(H_2O)_3]$, and (f) $Li_2[Zn_3Li_5(Btc)_4(Mtaz)(H_2O)_4]$. Reprinted with permission from [34]. Copyright © 2017 by the American Chemical Society.

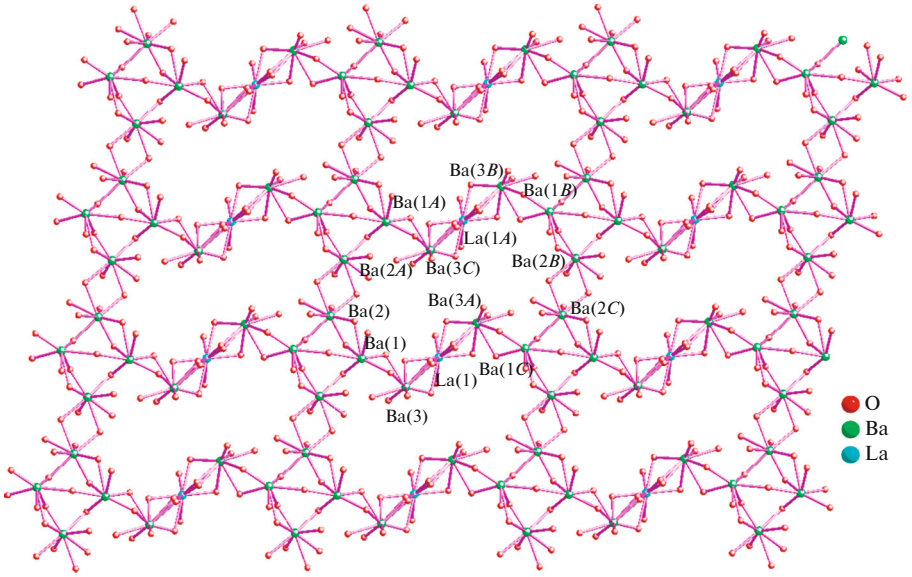

Fig. 9. Heterometallic cage of the structure of $[Ba_3La_{0.5}(\mu^3\text{-L})_{2.5}(H_2O)_3(DMF)] \cdot 3DMF$. Reprinted with permission from [35]. Copyright © 2016 by the American Chemical Society.

pounds were synthesized from nickel(II) nitrate and the corresponding Ln(III) acetates. The obtained compounds are microporous, can reversibly sorb carbon dioxide, and also demonstrate a high selectivity for the separation of CO_2/N_2 and CO_2/CH_4 mixtures (selectivity factor to 98.8 and 16.8, respectively, at 298 K and 100 kPa). The antiferromagnetic interactions for the MOF based on both Dy and Tb and the ferromagnetic interaction for Gd are observed at low temperatures due to the competition of the magnetic anisotropy and intermetallic ferromagnetic superexchange. In addition, the MOF based on Dy demonstrates a slow relaxation of magnetization at the zero dc field, whereas the Gd-based MOF demonstrates a significant cryogenic magnetocaloric effect with the maximum change in the entropy 26.6 J kg^{-1} K^{-1} at 3.0 K.

The heterometallic MOF $[NaEu_2(Tatab)_2(DMF)_3]$-OH (H_3Tatab is 4,4',4"-*s*-triazine-1,3,5-triyltri-*m*-aminobenzoic acid) was synthesized from europium(III) nitrate and Na_3Tatab [38]. The heterometallic node in the structure represents the hexacarboxylate trinuclear linear fragment $\{NaEu_2(COO)_6$-

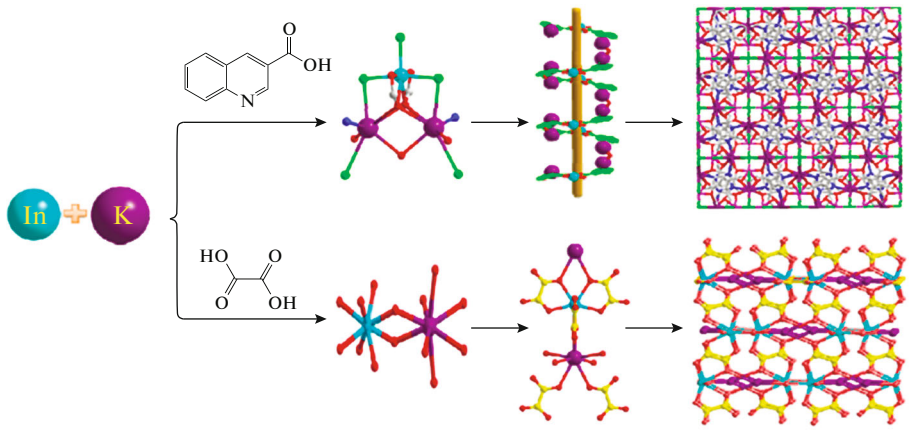

Fig. 10. General scheme of the synthesis and structures of the heterometallic MOF. Reprinted with permission from [36]. Copyright © 2016 by the American Chemical Society.

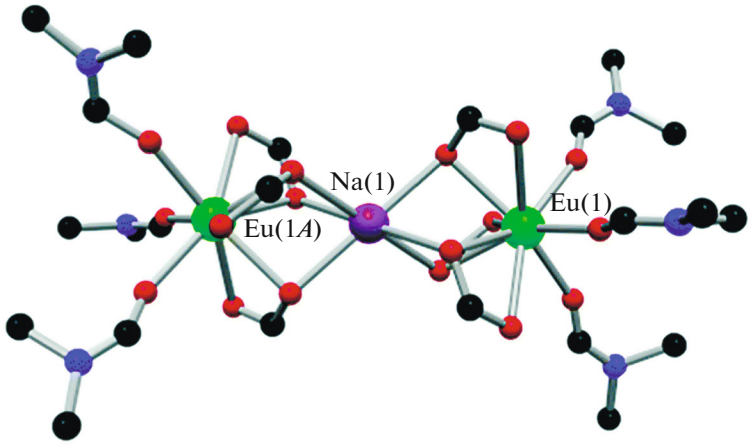

Fig. 11. Heterometallic node in the structure of $[NaEu_2(Tatab)_2(DMF)_3] \cdot OH$. Adapted from [38] with permission from the Royal Society of Chemistry.

$(DMF)_6\}$ (Fig. 11). The compound manifests a high hydrolytic stability. Experiments on the luminescence detection of antibiotics and various aromatic compounds were conducted. The luminescence quenching was observed upon the inclusion of ornidazole, nitrophenol, and benzyl alcohol.

The structures of two isostructural carcasses $[(CH_3)_2NH_2]_2[Zn_2Ln_2(Fda)_6(DMF)_2] \cdot 2DMF$ (Ln = Eu and Tb; H_2Fda is furan-2,5-dicarboxylic acid) contain the tetranuclear carboxylate node [39] (Fig. 12). In the three-dimensional structure, these nodes are linked into the bcu topology. The corresponding nitrates were used as sources of metal cations, and the synthesis was conducted in DMF under the solvothermal conditions. These MOF demonstrate an excellent stability in diverse solvents and are promising materials for the production of sensors for the fast and highly selective detection of aniline.

SYNTHESIS ON THE BASIS OF PRE-SYNTHESIZED HETEROMETALLIC COMPLEXES

The most propagated approach to the synthesis of heterometallic coordination polymers implies the use of a mixture of various metal salts, and heterometallic building blocks are formed *in situ* during the crystal growth. However, in many cases, these heterometallic building blocks are known as discrete polynuclear complexes with monotopic ligands. These complexes are highly soluble and fairly stable to retain the structure during the substitution of the monotopic ligand by the polytopic one for the formation of the polymeric structure of the compound. Thus, the synthesis of certain coordination polymers can be rationalized by choosing the corresponding pre-synthesized soluble polynuclear complex. In our opinion, the synthesis of the MOF from the pre-synthesized heterometallic complexes seems to be the most promising. In spite of

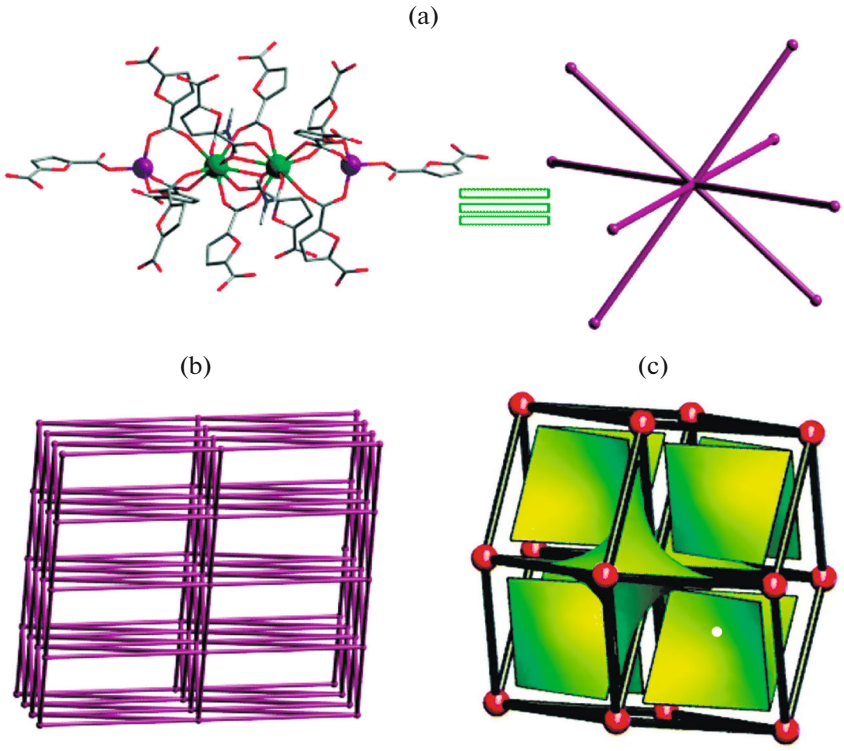

Fig. 12. (a) Eight-bonded node $\{Zn_2Ln_2(COO)_{10}\}$ in the Zn–Eu structure: Zn is violet, Eu is green, O is red, N is blue, and C is black; (b) bcu topology of the Zn–Eu structure; and (c) cavities in the structure. Reproduced from [39] with permission from the Royal Society of Chemistry.

obvious advantages from the viewpoint of the control and prediction of the structures and properties of the synthesized MOF, this approach is used rather rarely so far. There are only single similar examples in the literature, and the systematic study of using heterometallic molecular complexes as a source of heterometallic nodes in the MOF structure was not performed earlier. The recent review devoted to the known examples for this approach [40] mainly concerns, however, examples of using monometallic polynuclear complexes.

The original approaches to the synthesis of the heterometallic pivalate complexes were developed at the Laboratory of Chemistry of Coordination Polynuclear Compounds of the Institute of General and Inorganic Chemistry (Russian Academy of Sciences) and were applied further for the synthesis of coordination polymers. Among the most interesting examples are the trinuclear carboxylate complexes $[M_3O(RCOO)_6L_3]$ (Fig. 13) obtained for a wide series of metals. In this case, the polymeric structure can grow due to both the substitution of monotopic carboxylates by polytopic carboxylates and the use of electroneutral polytopic linkers capable of coordinating metal cations with the substitution of L. Moreover, the core is a good platform for the synthesis of numerous heterometallic complexes $[M'M_2O(RCOO)_6(L)_3]$) usually on the basis of the 3*d*-metal series. These complexes are very convenient initial materials for the rational design of heterometallic coordination polymers, and many such examples were successfully used at the Institute of General and Inorganic Chemistry (Russian Academy of Sciences).

It was proposed to use the polytopic donor bridging linkers of various geometry for linking the heterometallic pivalate complexes $[M'M_2O(Piv)_6(HPiv)_3]$ (Piv is $ButCOO^-$) in the targeted synthesis of MOF. Two isostructural coordination polymers $[Fe_2MO(Piv)_6(Bpy)_{3/2}]$ (M is Ni^{2+} or Co^{2+}) were synthesized due to

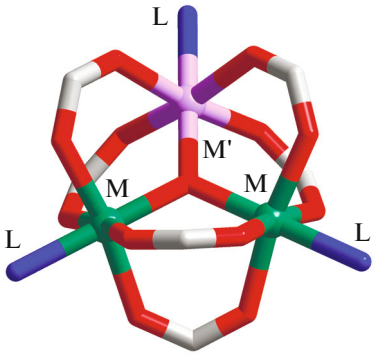

Fig. 13. Structure of the $[M'M_2O(RCOO)_6L_3]$ node.

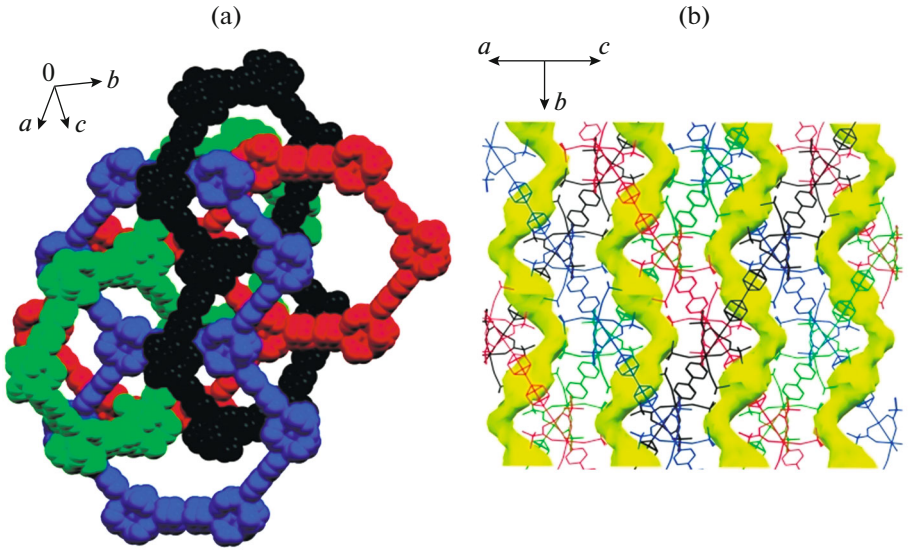

Fig. 14. (a) Intergrowth of the 2D layers (*t*-Bu groups of the pivalate anions and hydrogen atoms are omitted) and (b) visualization of the channels. Adapted with permission from [41]. Copyright © 2017 by Wiley-VCH.

linking the corresponding trinuclear heterometallic pivalates with the linear Bpy linkers [41]. The obtained layers with the **hcb** topology are packed into a porous intergrown structure with zigzag channels (Fig. 14). The microporous nature of these MOF was confirmed by the measurements of the N_2 and H_2 adsorption isotherms (S_{BET} = 520 m^2 g^{-1} for M = Ni, S_{BET} = 273 m^2 g^{-1} for M = Co).

The structures of the trinuclear heterometallic pivalate complexes are retained in the coordination polymers. The magnetic behavior of $[Fe_2MO(Piv)_6(Bpy)_{3/2}]$ is determined by the exchange interactions in the trinuclear blocks [42]. In addition, the crystal structures of the porous coordination polymers $[Fe_2MO(Piv)_6(Bpy)_{3/2}]$ turned out to be flexible from the viewpoint of changes in the distances between the layers, which resulted in a change in the pore volume. These changes are completely reversible and caused by the replacement of the solvent. A strong difference was found between the sorption of alkanes and alcohols: although the sorption isotherms of alkanes (*n*-hexane and *n*-octane) are typical of the microporous sorbents, the adsorption of alcohols (methanol and ethanol) was probably related to structural rearrangements. The higher sorption capacity for ethanol compared to that of methanol is consistent with the hydrophobic nature of the channels.

The $[Fe_2NiO(Piv)_6(Bpy)_{3/2}]$ complex was used for the preparation of a broad series of polymeric structures using various tritopic nitrogen-containing linkers [43, 44]. The obtained compounds demonstrated a permanent porosity for the isotherms of nitrogen and hydrogen sorption at 78 K. In addition, the porous coordination polymer $[Fe_2NiO(Piv)_6(L^2)]$ (L^2 is 4-(4-*N*,*N*-dimethylaminophenyl)-2,6-bis(4-pyridyl)pyridine) was used as a heterogeneous catalyst for the condensation of salicylaldehyde or 9-anthracenecarbaldehyde with malononitrile. The highest activity was observed in the case of salicylaldehyde, which resulted in its transformation into 2-imino-2*H*-chromene-3-carbonitrile in a high yield.

The binding of the fragment of the trinuclear complex $[Fe_2CoO(Piv)_6]$ via the redox-active bridge $[Ni(L^6)_2]$ (L^6H represents the Schiff base obtained from 4-pyridinecarboxylic acid hydrazide and 2-pyridinecarbaldehyde) gives the new porous coordination polymer $[\{Fe_2CoO(Piv)_6\}Ni(L^6)_2\}]^+$ [45]. The crystalline lattice of this compound is built of 2D layers, where each $[Ni(L_6)_2]$ ligand links two $[Fe_2CoO(Piv)_6]$ layers. The magnetic properties of the coordination polymer depend mainly on the magnetism of individual components (trinuclear pivalate and $[Ni(L_6)_2]$ bridge), since the interactions between these components are insignificant.

In the crystal structure of $[Li_2M_2(RCOO)_6L_2]$, each Li^+ cation exists in the tetrahedral environment, whereas each heavier metal can have the coordination number 4 or 5 depending on the nature of this metal and axial ligands L (Fig. 15). The highly developed coordination chemistry of these tetranuclear molecular complexes makes them attractive building blocks for the rational synthesis of heterometallic coordination polymers.

A broad series of new heterometallic MOF was obtained on the basis of such pivalate complexes. The most bright representatives of this class of compounds are two series of isoreticular carcasses $[LiM(Btb)(Solv)_2]$ (M = Zn^{2+} or Co^{2+}, and H_3Btb is 1,3,5-

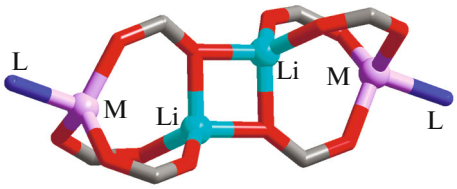

Fig. 15. Structure of the $[Li_2M_2(RCOO)_6L_2]$ node.

tris(carboxyphenylbenzene)) [46] and $[Li_2Zn_2(R\text{-}Bdc)_3(Bpy)]$ (R is the substituent in the terephthalate ligand) [47].

A series of layered and three-dimensional coordination polymers, where the tetranuclear fragment decomposes to two identical heterometallic tricarboxylate fragments $\{LiM(RCOO)_3\}$, was obtained [46, 48]. The use of tricarboxylate organic linkers of various geometries makes it possible to finely vary the dimensionality of the synthesized coordination polymers. In the case of the layered compounds, their structural stability increases substantially due to additional interactions between the aromatic systems of the linkers of the adjacent layers to form the so-called supramolecular 3D structure with one-dimensional channels (Fig. 16).

Owing to this stabilization, the $[LiM(Btb)(Solv)_2]$ compounds are fairly stable when guest molecules are removed and demonstrate the permanent porosity shown by the CO_2 sorption isotherms at 195 K. Since the channels turned out to be narrow, the compounds are of interest for the separation of such gas mixtures as CO_2/N_2 and CO_2/CH_4, because they do not sorb nitrogen and methane. It is noteworthy for the structures of the $[Li_2Zn_2(R\text{-}Bdc)_3(Bpy)]$ compounds that this is one of a few unique examples where both the geometry of the initial tetranuclear fragment is retained during the synthesis and all carboxylate linkers and monotopic donor pyridine linkers can be substituted by ditopic Bpy (Fig. 17). The three-dimensional structure contains a system of broad channels, whose diameter depends on the size of the substituent in the benzene ring of the terephthalate anion. In the case of the largest substituent (nitro group), some lateral channels turned out to be completely blocked transforming the system of channels into isolated one-dimensional channels. The compounds are permanently porous and have the surface area from 450 to 1200 m^2/g (measured by the BET method). Owing to the functionalization of the internal pore surface due to the use of the terephthalate anion with substituents in the benzene ring, the compounds can be used for the separation of various mixtures, including the industrially important separation of benzene and cyclohexane.

The work with the heterometallic complexes is being continued. The possibility of the use of other initial $\{M_2Ln\}$ fragments is shown [49]. This field of research seems impressively perspective, since it presents the possibility for the structural design of the new class of coordination polymers.

To conclude, the chemistry of the heterometallic MOF provides possibilities for the modification of the properties of the already known homometallic coordination polymers and also makes it possible to prepare new unique series of compounds with interesting sorption, optical, magnetic, and other functional properties. When using the pre-synthesized heterometallic complexes, the targeted synthesis of the MOF with the specified structure of the heterometallic core can be performed, and this substantially simplifies the preparation of new heterometallic MOF.

FUNDING

This work was supported by the Russian Foundation for Basic Research, project no. 18-33-00299.

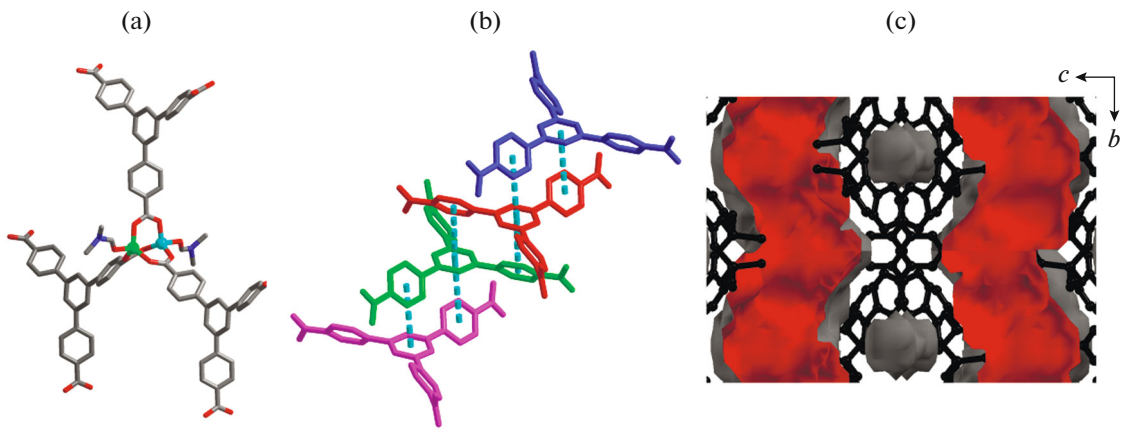

Fig. 16. (a) Secondary building block in $[LiZn(Btb)(DMF)_2]$, (b) stabilization of layers, and (c) visualization of the channels in the structure.

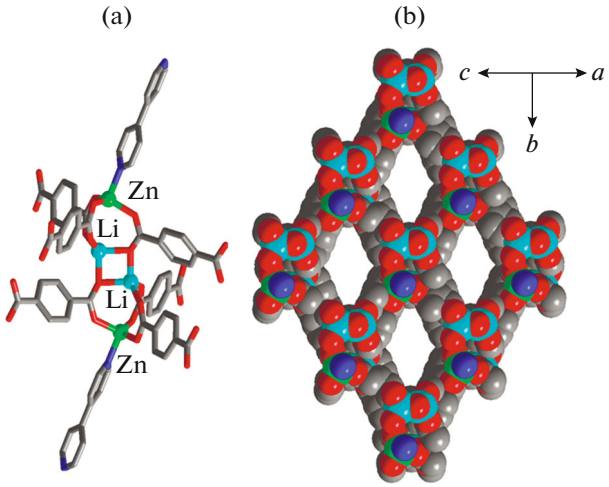

Fig. 17. (a) Secondary building block in the structure of $[Li_2Zn_2(Bdc)_3(Bpy)]$ [47] and (b) projection of the structure perpendicularly to the channels.

CONFLICT OF INTEREST

The authors declare that they have no conflicts of interest.

REFERENCES

1. Hoskins, B.F. and Robson, R., *J. Am. Chem. Soc.*, 1990, vol. 112, no. 4, p. 1546.
2. Barsukova, M.O., Sapchenko, S.A., Dybtsev, D.N., and Fedin, V.P., *Russ. Chem. Rev.*, 2018, vol. 87, no. 11, p. 1139.
3. Qin, J.-S., Yuan, S., Wang, Q., et al., *J. Mater. Chem. A*, 2017, vol. 5, no. 9, p. 4280.
4. Bunck, D.N. and Dichtel, W.R., *Chem.-Eur. J.*, 2013, vol. 19, no. 3, p. 818.
5. Burrows, A.D., *CrystEngComm*, 2011, vol. 13, no. 11, p. 3623.
6. Dhakshinamoorthy, A., Asiri, A.M., and Garcia, H., *Catal. Sci. Technol.*, 2016, vol. 6, no. 14, p. 5238.
7. Fei, H., Cahill, J.F., Prather, K.A., and Cohen, S.M., *Inorg. Chem.*, 2013, vol. 52, no. 7, p. 4011.
8. Yu, W., Porosoff, M.D., and Chen, J.G., *Chem. Rev.*, 2012, vol. 112, no. 11, p. 5780.
9. Sun, N.-N. and Yan, B., *Analyst*, 2018, vol. 143, p. 2349.
10. Sun, N. and Yan, B., *Phys. Chem. Chem. Phys.*, 2017, vol. 19, p. 9174.
11. Hao, J.-N., Xu, X.-Y., Lian, X., et al., *Inorg. Chem.*, 2017, vol. 56, no. 18, p. 11176.
12. Perfecto-Irigaray, M., Albo, J., Beobide, G., et al., *RSC Adv.*, 2018, vol. 8, no. 38, p. 21092.
13. Sapchenko, S.A., Demakov, P.A., Samsonenko, D.G., et al., *Chem.-Eur. J.*, 2017, vol. 23, no. 10, p. 2286.
14. Cheng, X., Jiang, Z., Cheng, X., et al., *J. Membr. Sci.*, 2018, vol. 545, p. 19.
15. Lü, Y., Jiang, Y., Zhou, Q., et al., *J. Solid State Chem.*, 2017, vol. 256, p. 93.
16. Du, J.-J., Zhang, X., Zhou, X.-P., and Li, D., *Inorg. Chem. Front*, 2018, vol. 5, no. 11, p. 2772.
17. Zhou, X.-P., Li, M., Liu, J., and Li, D., *J. Am. Chem. Soc.*, 2012, vol. 134, no. 1, p. 67.
18. Wu, Y., Zhou, X.-P., Yang, J.-R., and Li, D., *Chem. Commun.*, 2013, vol. 49, no. 33, p. 3413.
19. Rubio-Giménez, V., Waerenborgh, J.C., Clemente-Juan, J.M., and Martí-Gastaldo, C., *Chem. Mater.*, 2017, vol. 29, no. 15, p. 6181.
20. Guo, W., Xia, W., Cai, K., et al., *Nano Micro Small*, 2017, vol. 13, no. 41, p. 1.
21. Bratsos, I., Tampaxis, C., Spanopoulos, I., et al., *Inorg. Chem.*, 2018, vol. 57, no. 12, p. 7244.
22. Li, C., Tang, H., Fang, Y., et al., *Inorg. Chem.*, 2018, vol. 57, no. 21, p. 13912.
23. Muldoon, P.F., Liu, C., Miller, C.C., et al., *J. Am. Chem. Soc.*, 2018, vol. 140, no. 20, p. 6194.
24. Béziau, A., Baudron, S.A., Fluck, A., and Hosseini, M.W., *Inorg. Chem.*, 2013, vol. 52, no. 24, p. 14439.
25. Han, Y., Sinnwell, M.A., Teat, S.J., et al., *Adv. Sci.*, 2019, vol. 6, no. 7, p. 1802056.
26. Abedi, M., Mahmoudi, G., Kirillov, A.M., and Kaminsky, W., *Polyhedron*, 2018, vol. 142, p. 110.
27. Ding, Y.-J., Li, T., Hong, X.-J., et al., *CrystEngComm*, 2015, vol. 17, no. 21, p. 3945.
28. Li, Y.-F., Wang, D., Liao, Z., et al., *J. Mater. Chem.*, 2016, vol. 4, no. 19, p. 4211.
29. Li, Q., Zhu, Z., and Qian, J., *Polyhedron*, 2018, vol. 155, p. 218.
30. Han, Y., Zheng, H., Liu, K., et al., *ACS Appl. Mater. Interfaces*, 2016, vol. 8, no. 35, p. 23331.
31. Hu, H.-C., Kang, X.-M., Cao, C.-S., et al., *Chem. Commun.*, 2015, vol. 51, no. 54, p. 10850.
32. Zhai, Q.-G., Bu, X., Mao, C., et al., *J. Am. Chem. Soc.*, 2016, vol. 138, no. 8, p. 2524.
33. Zhou, W. and Huang, D.D., Wu, Y.P., et al., *Angew. Chem., Int. Ed. Engl.*, 2019, vol. 51, no. 13, p. 4227.

34. Li, Y.-P., Wang, X.-X., Li, S.-N., et al., *Cryst. Growth Des.*, 2017, vol. 17, no. 11, p. 5634.
35. Ding, B., Liu, S.X., Cheng, Y., et al., *Inorg. Chem.*, 2016, vol. 55, no. 9, p. 4391.
36. Du, X., Fan, R., Wang, X., et al., *Cryst. Growth Des.*, 2016, vol. 16, no. 3, p. 1737.
37. Feng, D.-D., Dong, H.-M., Liu, Z.-Y., et al., *Dalton Trans.*, 2018, vol. 47, no. 43, p. 15344.
38. Han, M.-L., Wen, G.-X., Dong, W.-W., et al., *J. Mater. Chem.*, 2017, vol. 5, no. 33, p. 8469.
39. Li, L., Zou, J.-Y., You, S.-Y., et al., *Dalton Trans.*, 2017, vol. 46, no. 47, p. 16432.
40. Dybtsev, D.N., Sapianik, A.A., and Fedin, V.P., *Mendeleev Commun.*, 2017, vol. 27, no. 4, p. 321.
41. Polunin, R.A., Kolotilov, S.V., Kiskin, M.A., et al., *Eur. J. Inorg. Chem.*, 2010, vol. 32, p. 5055.
42. Polunin, R.A., Kolotilov, S.V., Kiskin, M.A., et al., *Eur. J. Inorg. Chem.*, 2011, vol. 32, p. 4985.
43. Dorofeeva, V.N., Kolotilov, S.V., Kiskin, M.A., et al., *Chem.-Eur. J.*, 2012, vol. 18, p. 5006.
44. Sotnik, S.A., Polunin, R.A., Kiskin, M.A., et al., *Inorg. Chem.*, 2015, vol. 54, p. 5169.
45. Lytvynenko, A.S., Kolotilov, S.V., Kiskin, M.A., et al., *Inorg. Chem.*, 2014, vol. 53, p. 4970.
46. Sapianik, A.A., Kiskin, M.A., Kovalenko, K.A., et al., *Dalton Trans.*, 2019, vol. 48, p. 3676.
47. Sapianik, A.A., Zorina-Tikhonova, E.N., Kiskin, M.A., et al., *Inorg. Chem.*, 2017, vol. 56, no. 3, p. 1599.
48. Sapianik, A.A., Kiskin, M.A., Samsonenko, D.G., et al., *Polyhedron*, 2018, vol. 145, p. 147.
49. Sapianik, A.A., Lutsenko, I.A., Kiskin, M.A., et al., *Russ. Chem. Bull.*, 2016, vol. 65, no. 11, p. 2601.

Translated by E. Yablonskaya